Modeling SARS-CoV-2 Infection Risk in Various Office Building HVAC Systems

BY ALBERTO CAVALLINI, FELLOW ASHRAE, FILIPPO BUSATO, PH.D., MEMBER ASHRAE, AND FABRIZIO PREGLIASCO

The SARS-CoV-2 pandemic aroused great interest in the HVAC community regarding both the design of new systems and management and operation strategies for existing ones. Risk management plays a key role in all-air systems, which are based on air recirculation among all spaces, and also in primary air systems. Following an explanation of the analytical approach, this article assesses the infection risk in several HVAC system layouts. It takes into account the role of air renewal (ventilation) and recirculation and the lowering of infection risk due to virus removal or inactivation (through mechanical or electrostatic filtration or inactivation technologies such as UV-C irradiation and ionization), with special attention to the management of airflows depending on plant layout.

The outbreak of the SARS-CoV-2 pandemic during the winter of 2019–20 drew immediate and special attention to HVAC systems and their possible contribution to the spread of the virus. In the beginning there was great doubt that the virus could spread via airborne transmission.[1] Now it is known for certain to be airborne, although there are other mechanisms of viral propagation. A 2018 review study highlights how different factors such as ventilation rates, direction of airflows and relative position of susceptible and infected individuals can affect the probability of infection by airborne droplets in the indoor environment.[2]

To assess the risk to individuals being infected by the pandemic virus, one must refer to an infection model for aerosol-carried particles. According to current knowledge about SARS-CoV-2, the most suitable model is the Wells-Riley model,[3] as widely supported

Alberto Cavallini is a professor emeritus, University of Padova - Manens SpA. Filippo Busato, Ph.D., is an associate professor at Universitas Mercatorum in Rome. Fabrizio Pregliasco is an associate professor at the Università Statale di Milano.

This peer-reviewed article does not represent official ASHRAE guidance. For more information on ASHRAE resources on COVID-19, visit ashrae.org/COVID19.

by recent literature.[4] The present work, by means of mass and concentration balance of airflows in HVAC systems, calculates the pathogen concentration, the resultant infection probability and the number of potentially infected individuals for different space layouts of segregated rooms served by the same HVAC system. Airflows and the number of people in the room are presumed steady state, while virus concentration is time dependent.

The main purpose of this work is to help build a conscious risk assessment plan for HVAC systems for designers, manufacturers, building owners and building managers.

Model and Input Data

According to the Wells-Riley model,[4] the probability for a susceptible individual to contract a disease via aerosol infection follows a Poisson probability function given by *Equation 1*:

$$P = 1 - e^{-p \cdot \int_0^T C_I(t)\,dt} \quad (1)$$

where

P = probability of infection of any exposed susceptible individual, a real number in the interval [0, 1]

$p \cdot \int_0^T C_I(t)\,dt$ = number of infectious quanta inhaled by a susceptible individual during the exposure time T, quanta

p = pulmonary inhalation rate of a susceptible individual, m^3/h

T = total time of exposure, h

$C_I(t)$ = instantaneous volume concentration at time t of infectious quanta in the environment (considered well mixed), quanta/m^3

Gammaitoni and Nucci derive an expression for calculating the viral concentration C_I given the following simplifying assumptions: the quanta emission rate q is considered constant over time, the latent period of the disease is longer than the time scale of the model and the droplets are distributed instantaneously and uniformly in the room.[5] This equation, which considers all vectors of viral load removal in the room volume (inactivation, deposition and ventilation), is as follows:

$$C_I = \frac{q \cdot I}{N \cdot V} + \left(\frac{n_0}{V} - \frac{q \cdot I}{N \cdot V} \right) \cdot e^{-N \cdot t} \quad (2)$$

where

q = infectious quanta emission rate by one asymptomatic infected individual, quanta h^{-1}

I = number of asymptomatic infected individuals

N = total virus removal rate in space, $N = \lambda + k + rn$, h^{-1}

λ = viral inactivation rate in space, h^{-1}

k = viral particle deposition (gravitational settling) rate in space, h^{-1}

rn = air renewal (outdoor air exchange) rate, h^{-1}

V = room volume, m^3

n_0 = initial level (at $t = 0$) of infectious quanta present in volume V, quanta

t = time, h

For $n_0 = 0$, *Equations 1* and *2* yield *Equation 3* for the probability of infection P:

$$P = 1 - \exp\left[\frac{q \cdot I \cdot p}{V} \left(\frac{1 - N \cdot T - e^{-N \cdot T}}{N^2} \right) \right] \quad (3)$$

This paper applies this model (with all connected assumptions, particularly well-mixed environments) in simulating some HVAC layouts of office buildings. The level of activity of all involved individuals is assumed to be in the category "speaking during light activity."

Please see online materials and I-P versions of the equations and related nomenclature for this article at tinyurl.com/JournalExtras.

Quanta Emission Rate Input Data

Among all the input parameters required for the application of the above model (*Equations 1* through *3*), the infectious quanta emission rate q of an asymptomatic infected individual related to the SARS-CoV-2 virus is unquestionably the most uncertain and controversial one, with a huge range.

At present, the only available data specifically related to the original SARS-CoV-2 virus come from a single group of authors, Buonanno et al.[4,6] These authors propose "a forward emission approach to estimate the quanta emission rate of an infected individual on the basis of viral load in the sputum and the concentration of droplets expired during different activities."[4] They analyze the worst-case scenario in the presence of an asymptomatic SARS-CoV-2–infected individual in several microenvironments: a pharmacy, a supermarket, a restaurant, a

FIGURE 1 Sketch of a multiroom HVAC plant with air recirculation.

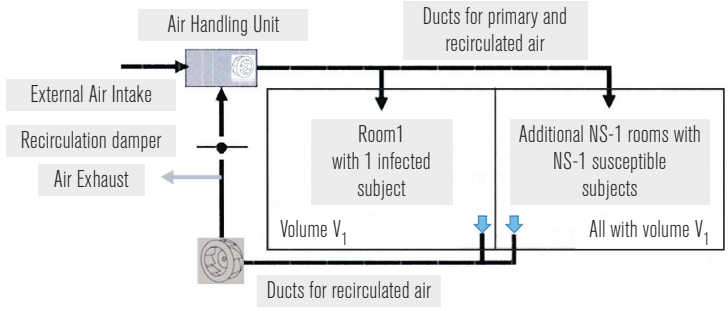

SOURCE: AICARR

FIGURE 2 Probability of infection for each asymptomatic individual after 8 h.

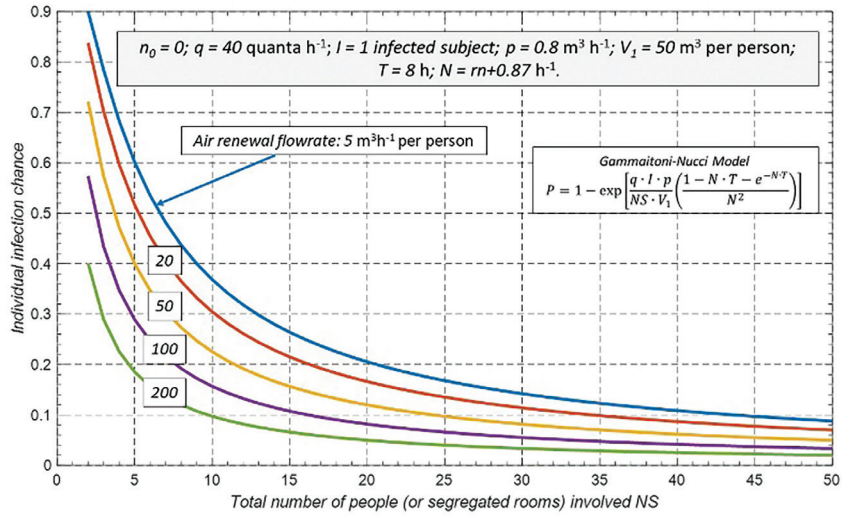

FIGURE 3 Number of susceptible individuals infected after 8 h.

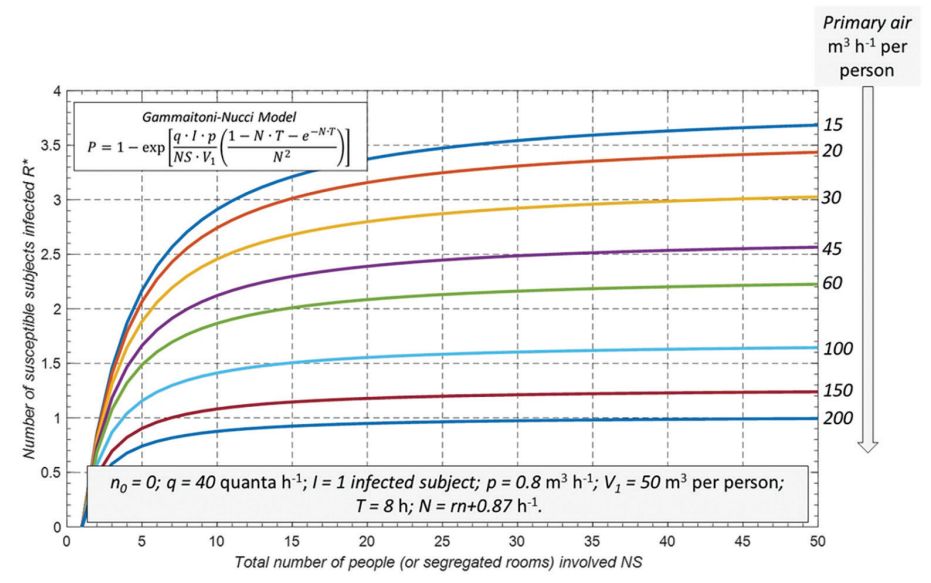

post office and a bank.[4] In that article, the value assumed for the quanta emission rate is q = 142 quanta h^{-1}, associated with pulmonary rate p = 0.96 m^{3}h^{-1} (0.57 cfm).[6] In a preprint version of the same article, the value assumed for the quanta emission rate is q = 147 quanta h^{-1}, associated with pulmonary rate p = 0.54 m^{3}h^{-1} (0.32 cfm).

In subsequent work, the same authors presented a novel approach for quantitative assessment of the infection risk based on the determination, through Monte Carlo simulations, of the probability density functions of quanta emission rate q, of quanta concentration C_I and of infectious quanta inhaled by a susceptible individual.[6] For a simplified estimate such as the one used in this work, they suggest adopting for the asymptomatic infected individual's quanta emission rate the 66th percentile of the quanta emission rate q of their probability density function. The 66th percentile q values for oral breathing during resting, oral breathing during heavy activity, speaking during light activity and singing (or loudly speaking) during light activity are 0.72, 4.9, 9.7 and 62 quanta h^{-1}, respectively.[6]

In the same paper, Buonanno et al. make a retrospective assessment of two documented COVID-19 outbreaks: in a restaurant in Guangzhou, China, and at a choir rehearsal in the Skagit Valley in Washington State, US.[6] In the restaurant outbreak, the backward calculation of the contagious individual's quanta emission rate yields q = 61 quanta h^{-1}; this value is above the 93rd percentile value (57.6 quanta h^{-1}) of

FIGURE 4 Diagram of segregated model.

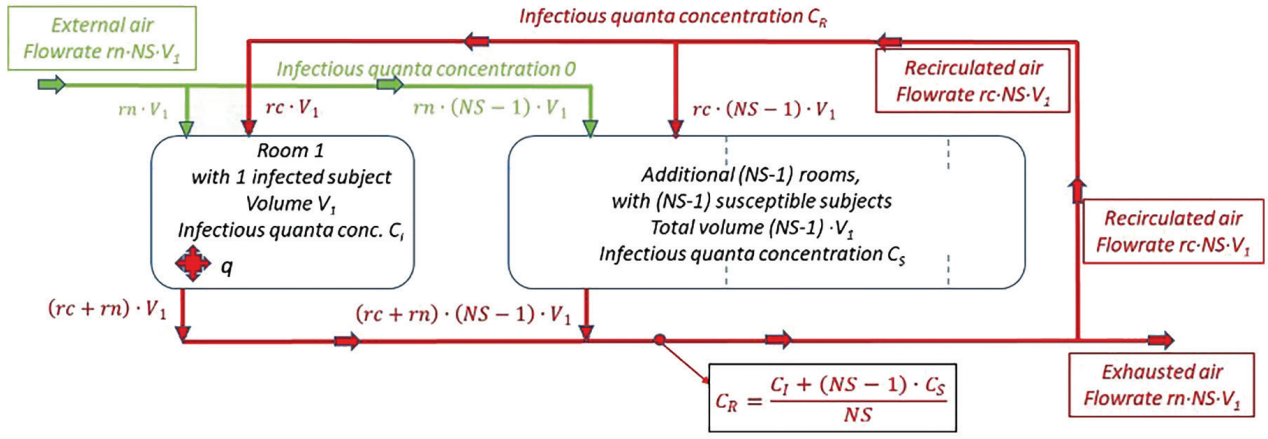

FIGURE 5A Number of susceptible individuals infected after 8 h (with $q = 40$ quanta h^{-1}).

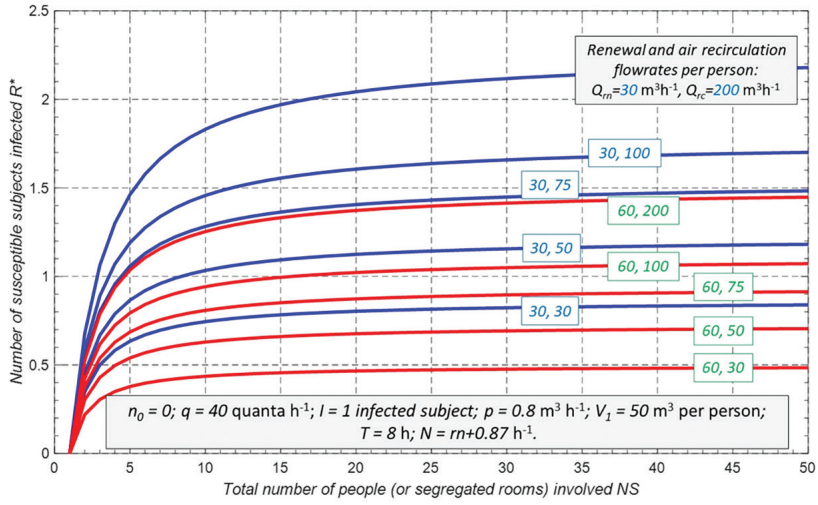

FIGURE 5B Number of susceptible individuals infected after 8 h (with $q = 120$ quanta h^{-1}).

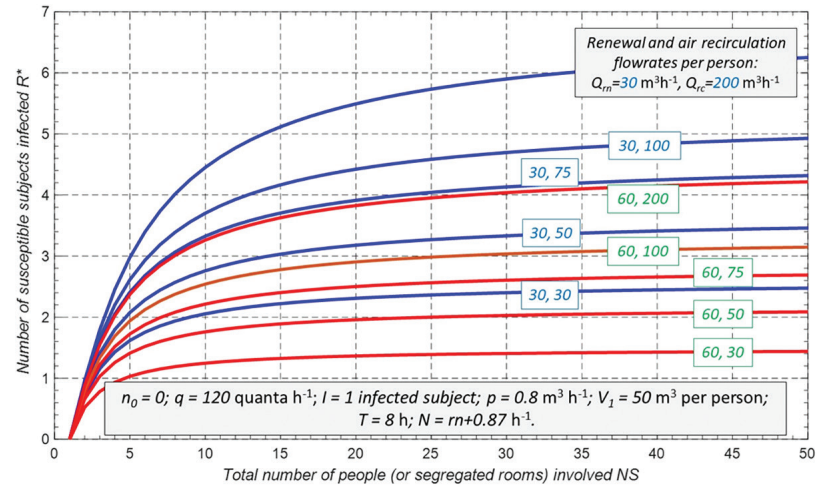

the probability density function of q for an emitting individual speaking during light activity. In the case of the choir rehearsal, the backward calculation yields q = 341 quanta h^{-1}, a value above the 92nd percentile (325 quanta h^{-1}) of the probability density function of q for an infected individual while singing. These examples show that the 66th percentile value of the probability density function of q of the Buonanno, et al., Monte Carlo analysis not only is far from a worst-case scenario, but likely also leads to values that are too small to represent baseline cases, even though it is based on the lower transmissibility of the original SARS-CoV-2 virus.

According to Jimenez and Peng, again referring to the original SARS-CoV-2 virus in Wuhan, China, for speaking during light exercise the coherent value is q = 13.2 quanta h^{-1} (to highlight the strong dependence of this parameter on activity level, the value suggested for loudly speaking during light exercise is q = 85 quanta h^{-1}, while for oral breathing during light exercise, q = 2.8 quanta h^{-1}).[7] The same authors suggest a multiplying factor of 3.3

for the Omicron BA.2 virus variant;[7] since the start of the SARS-CoV-2 pandemic in late 2019, several variants of concern have been reported to have increased transmissibility.

Taking into account all of the data and considerations presented above, all simulations presented below assume the quanta emission rate of an asymptomatic infected individual to be q = 40 quanta h^{-1}, a value considered more appropriate in the present situation than can be directly inferred from Buonanno et al.[6] In addition, a couple of simulations were repeated with the value of q elevated to 120 quanta h^{-1}, both to account for the large uncertainty of these data and to show the sensitivity of the results to this parameter.

FIGURE 6 Effect of different removal/inactivation efficiencies.

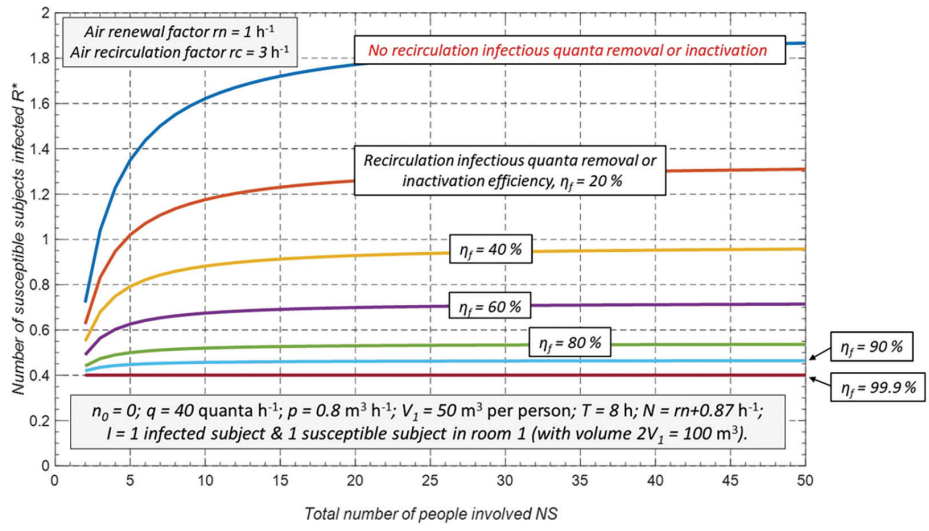

FIGURE 7 Effect of different air recirculation rates with a removal/inactivation efficiency of 40%.

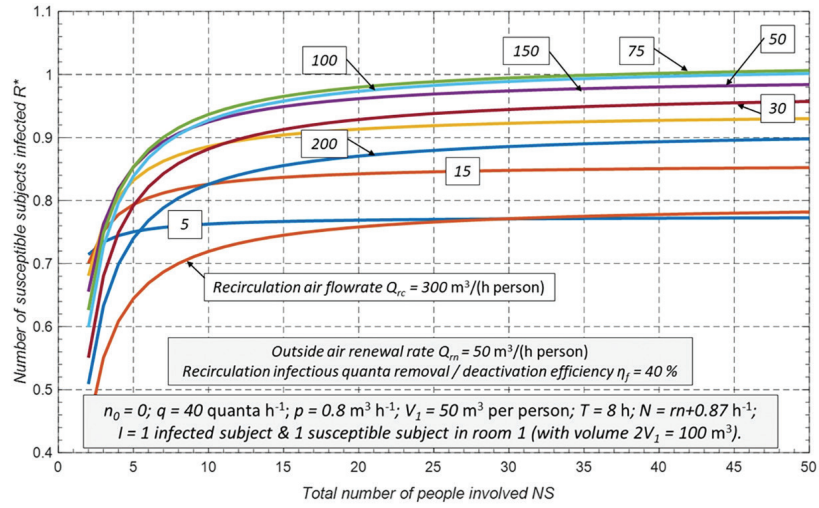

Other Input Data

As to the pulmonary inhalation rate p, Adams (as reported in Buonanno et al.[4]) gives the following values, averaged between male and female individuals: 0.49 m^{3}h^{-1} (0.29 cfm) for resting, 0.54 m^{3}h^{-1} (0.32 cfm) for standing, 1.38 m^{3}h^{-1} (0.81 cfm) for light exercise, 2.35 m^{3}h^{-1} (1.38 cfm) for moderate exercise and 3.30 m^{3}h^{-1} (1.94 cfm) for heavy exercise. All the simulations reported in this work adopt the conservative value p = 0.8 m^{3}h^{-1} (0.5 cfm).

Regarding the removal contribution factors λ (due to viral inactivation in the space) and k (due to gravitational settling), again the values assumed in the simulations illustrated below comply with the data from Buonanno et al.: λ = 0.63 h^{-1} (based on SARS-CoV-2 half-life of 1.1 h) and k = 0.24 h^{-1} (based on an emission source height of 1.5 m [4.9 ft]);[4] consequently, the total virus removal rate is expressed as N = λ + k + rn = rn + 0.87 h^{-1}. Finally, the values assumed for the air recirculation rate rc and the virus-free air renewal (outdoor air exchange) rate rn comply with current design practice; the extreme values can demonstrate the trend of the simulation results.

Due to the high uncertainty of some of the input data (for the quanta emission rate q probably even at factor of 5), readers are advised to look at the simulation's numerical results with caution. At this stage of knowledge of this particular virus, it is far more important to look at the trends and variations of the simulation results as the input parameters and control measures vary.

The results reported below refer to the probability

FIGURE 8 Effect of the outdoor air renewal rate for different removal/inactivation efficiencies (with $q = 120$ quanta h^{-1}).

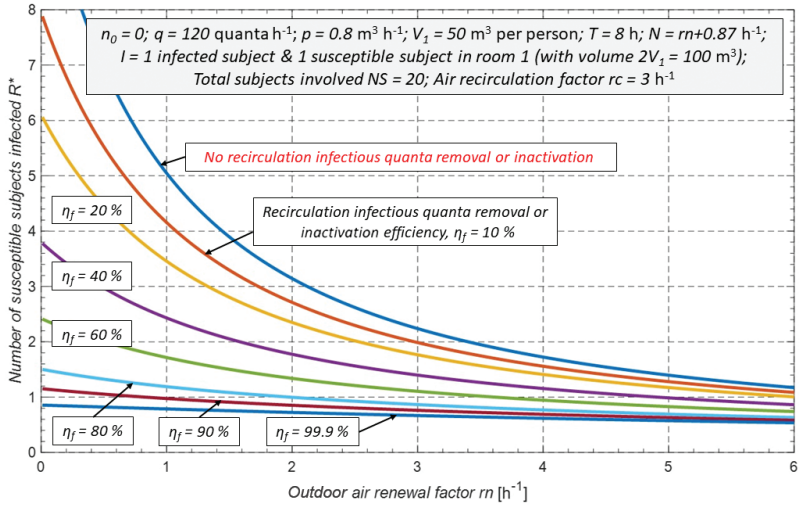

FIGURE 9 Effect of the air recirculation rate for different removal/inactivation efficiencies.

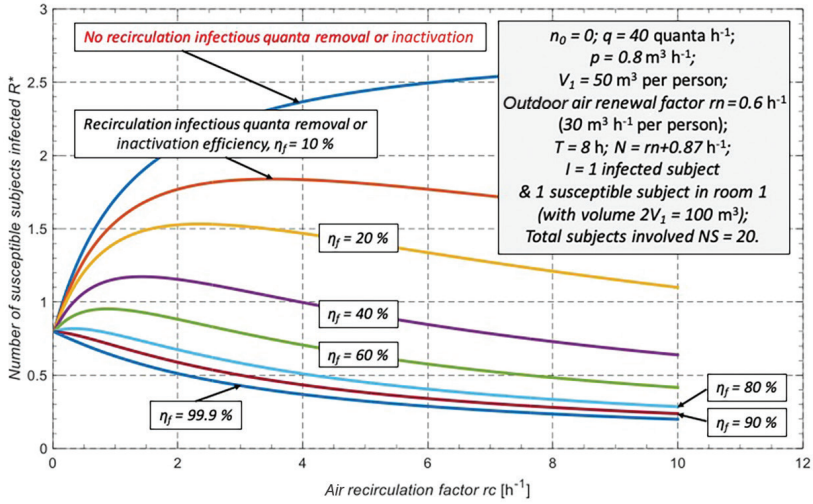

of infection of susceptible individuals; in the case of the current SARS-CoV-2 pandemic, it must be considered that all vaccines currently in use protect, even if only partially, against infection and onward transmission. However, this study, although focused on the current SARS-CoV-2 pandemic, aims to develop a preemptive plan for HVAC management of future pandemics caused by novel viruses.

All-Air Multiroom AC Plants with Air Recirculation

The sketch in *Figure 1* represents an office building multiroom AC all-air plant with air recirculation among the *NS* separated rooms, each of volume $V_1 = 50$ m^3 (1,800 ft^3) and each with a single occupant. Room 1 accommodates an asymptomatic contagious individual, while in the remaining $NS - 1$ rooms $NS - 1$ susceptible individuals are equally distributed. All individuals stay in their offices for $T = 8$ h. At this point the simulation assumes that air recirculation brings about no additional removal or inactivation of the infectious quanta.

To model the spreading of the disease in this situation, one can employ two different models, here dubbed the *uniform model* and the *segregated model*, as illustrated below.

Uniform Model

It can be assumed that the effect of the air recirculation among all rooms is equivalent to eliminating the partitions separating the different spaces: all rooms can be treated together as a single well-mixed space of total volume $V = NS \cdot V_1$, and so *Equations 2* and *3* can be directly applied to this total volume. *Figures 2 and 3* and *Online Figure 1* illustrate the results of this procedure as a function of the number of rooms (or the number of people) *NS* involved.

Online Figure 1 gives the number of infectious quanta inhaled by any susceptible individual during the 8 h working period, showing the dependence of this quantity on the fresh (outdoor) air renewal volumetric airflow rate per person Q_{rn}. *Figure 2* reports the corresponding infection probability *P* for any exposed susceptible individual. Finally, *Figure 3* shows the reproduction index $R^* = P \cdot (NS - 1)$, the total number of people potentially infected. This index always increases with the number of individuals involved, although the probability of infection for any susceptible individual decreases when the total number of people involved increases.

The uniform model faces some strong limitations: it considers the environment as a single room, with

no difference in infectious quanta concentration between the room with the infected individual and the other spaces. This condition calls for infinite internal air recirculation—the only way to guarantee

FIGURE 10 Diagram of multiroom layout with ventilation/primary air system, including common spaces.

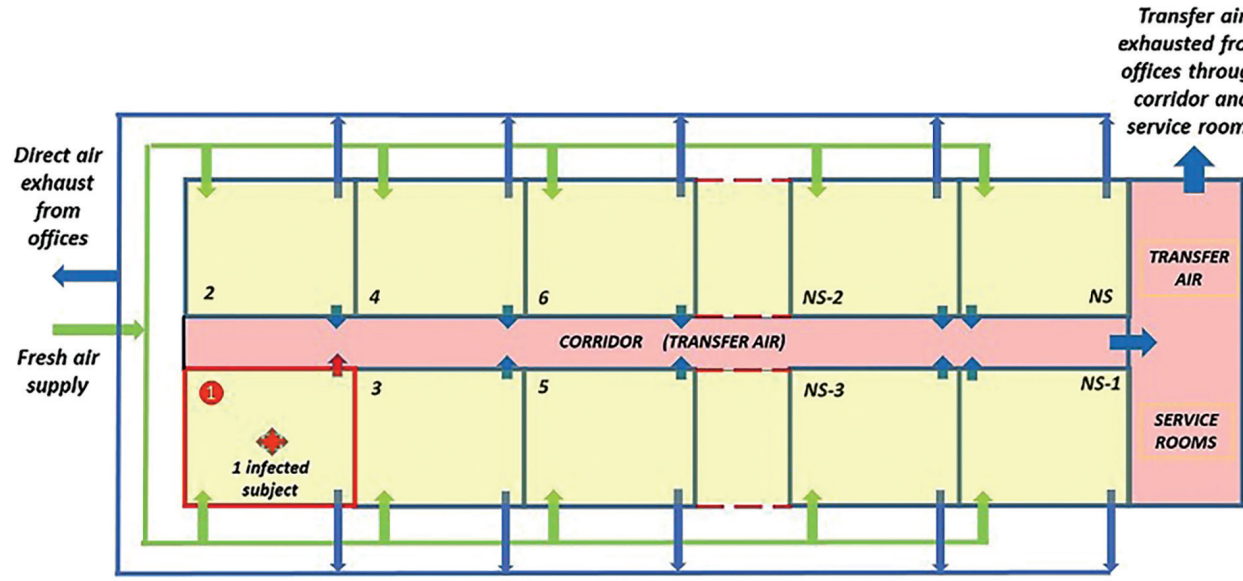

the "well-mixed" conditions among all the rooms. It clearly represents a limit case, when the air recirculation rate is much higher than the outdoor air exchange (renewal) rate ($rc >> rn$).

FIGURE 11 Concentration of infectious quanta in the corridor and service rooms.

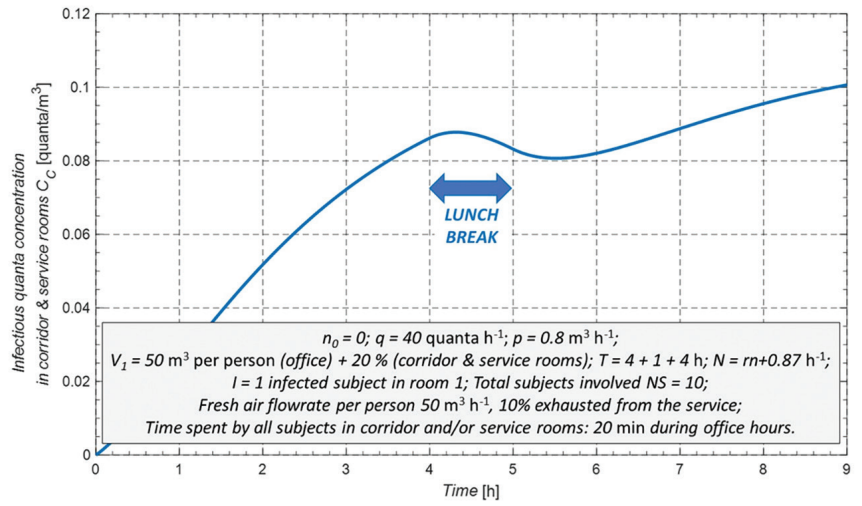

Segregated Model

A big step forward in the segregated model is retaining physically segregated spaces; the only connection among different rooms is given by the all-air ducted HVAC plant, providing airflows with rn (h^{-1}) as the renewal rate and rc (h^{-1}) as the recirculation rate in each room. *Figure 4* shows a diagram of this model. The diagram does not exactly reproduce the actual system configuration, which generally involves recirculated air being mixed with outdoor air to form supply air before introduction into rooms. However, this schematic makes it easier to understand how the equations are derived and leads to the same result as the actual situation regarding viral concentration in the rooms.

Equation 4 refers to the concentration of infectious quanta in the infected room, while *Equation 5* refers to that of the other rooms. All spaces are considered perfectly mixed.

$$\frac{dC_I}{dt} = \frac{q \cdot I}{V_1} + rc \cdot C_R - (rc + N) \cdot C_I \quad (4)$$

$$\frac{dC_S}{dt} = rc \cdot C_R - (rc + N) \cdot C_S \quad (5)$$

$$C_R = \frac{C_I + (NS - 1) \cdot C_S}{NS} \quad (6)$$

where

C_I = volume concentration of infectious quanta in the infected room, quanta/m^3

rc = air recirculation rate, h^{-1}

C_R = volume concentration of infectious quanta in the recirculated air, quanta/m^3

C_S = volume concentration of infectious quanta in susceptible individuals' rooms, quanta/m^3

NS = total number of people involved (asymptomatic infected individuals + susceptible individuals)

Including *Equation 6* in the model yields a first-order ordinary differential algebraic equation (ODAE) system reducible to a symbolically solvable ordinary differential equation (ODE) system, whose explicit solution is omitted for the sake of brevity. The system can be numerically solved by a code in a suitable computing environment.

Figures 5a (for q = 40 quanta h^{-1}) and *5b* (for q = 120 quanta h^{-1}) show the results of the application of the segregated model in terms of the reproduction index R^* versus the total number of people involved NS. The dependence of R^* on both the fresh (outdoor) air renewal volumetric airflow rate per person Q_{rn} and the air recirculation volumetric airflow rate per person Q_{rc} is evident in both figures.

Effect of Virus Removal/Inactivation in the Supply Duct

It is also possible to extend the segregated model in order to account for the presence of filtration or inactivation devices (high-efficiency mechanical or electrostatic filters, UV-C irradiation, photocatalytic oxidation, negative air ionization or other similar technologies) in the air supply duct after the mixing plenum. Assuming a removal/inactivation efficiency η_f in the interval [0, 1], a multiplication factor of (1-η_f) must be introduced in the C_R formula in *Equation 6*. *Figures 6, 7, 8* and *9* and *Online Figure 2* show, for the

FIGURE 12 Susceptible individuals infected as a function of the time all persons spend in the common spaces.

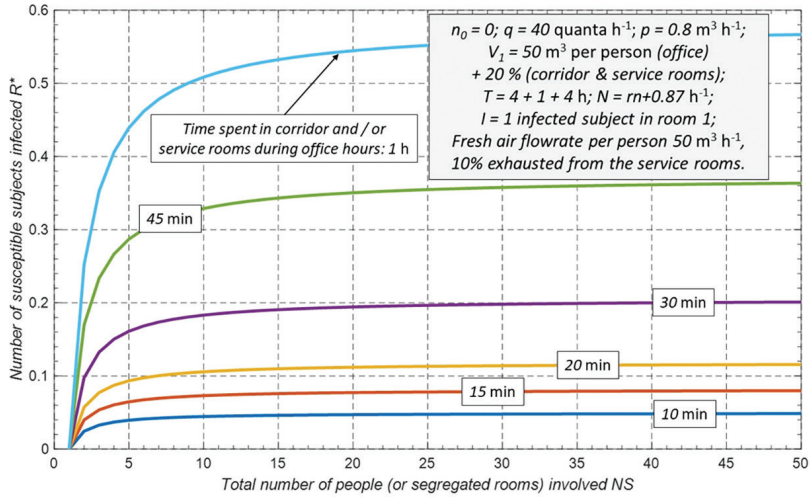

FIGURE 13 Susceptible individuals infected as a function of air renewal and of the fraction of air extracted from the common spaces.

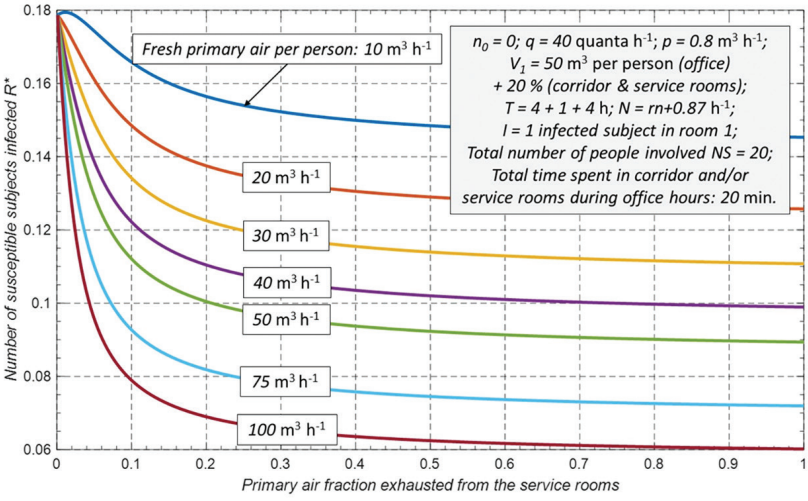

case of double-occupancy rooms, the effect of virus removal/inactivation on all exposed subjects. As seen in the plot labels in *Figures 6, 7, 8 and 9 and Online Figure 2*, the case refers to two people in room 1 (one infected and one susceptible person) of volume $2V_1$, while the other *NS* – 2 people are segregated in the other rooms; each individual again has at his disposal a volume V_1 = 50 m^3 (1800 ft^3). Therefore the number of potentially infected individuals includes one susceptible individual in room 1 and *NS* – 2 susceptible individuals in the remaining rooms; because of the presence of the infector's roommate, *R** cannot reach 0 even for *rc* = 0.

It is interesting to observe that, in the case illustrated in *Figure 7*, the reproduction index *R** reaches a maximum as the air recirculation rate increases to 75 m^3 h^{-1} person^{-1} (44 cfm/person) and then decreases at higher recirculation rates. This result, also evident in *Figure 9* for removal/inactivation efficiencies less than 80%, is due to the double, contrasting effect of increasing air recirculation when air purification devices are present in the supply ducts. On one hand, air recirculation spreads the virus to the rooms occupied by the susceptible individuals; on the other hand, the device in the air-handling system remove/inactivate the virus content in all the rooms.

Note that the same results on the risk of infection are obtained with the installation of the viral filtration/inactivation device on the recirculated air fraction only, with a smaller flow rate than the total supply flow rate, given the assumption of no virus in the outdoor fresh air.

Common Spaces Ventilation Management

By suitable adaptation of *Equations 3*, *4* and *5*, it is possible to extend the segregated model to specific real-world applications and to consider common spaces and a likely scheduling for room occupation as well. *Figure 10* shows the situation where, in addition to *NS* single-occupancy offices, there are common spaces (corridor, service rooms) with a volume amounting to 20% of the total volume of the offices served by the primary air HVAC plant. It must be noted that this is not an all-air plant, but a ventilation/primary air system. The infected individual is in room 1 and, along with his workmates, spends a fraction of the working time (8 h per day) in the common areas. In addition, all the occupants leave the building for a 1 h

lunch break after 4 h in the building in the morning and come back for 4 h in the afternoon. An exhaust fan in the service rooms extracts the transfer air, while the air-handling unit supplies the full 100% outdoor fresh air to the single offices only; there is no direct supply air to the corridor or to the service rooms.

The system in this example case has hydronic local terminals and primary air supplied by a ducted handling unit to the individual offices, with heat recovery from the ducted exhaust air without recirculation. To prevent the propagation of offensive odors or other pollutants from certain rooms (toilet service, copier room, etc.), a fraction of the total ventilation air is expelled outside directly from the rooms, independently of the general extraction system, thus generating an appropriate pressure gradient in the building.

Online Figure 3 shows a timeline of the infectious quanta concentration in the room of the infected individual C_I, while *Figure 11* shows the timeline of quanta concentration in the well-mixed common spaces (corridor, service rooms) C_C. It is assumed that the infected person and the other workers spend 20 min during the whole working time in the common spaces (20 min in two 4 h periods); the plots refer to a total number of people involved $NS = 10$, an air renewal rate $rn = 1\ h^{-1}$, and 10% ventilation air exhausted from the common rooms.

Figure 12 shows how the presence of the infected individual in the common spaces and the fraction of ventilation air exhausted from the service rooms affect the number of susceptible people expected to be infected during the working day R^*. *Figure 13* shows how increasing the fraction of air extracted from the common spaces can actively reduce the number of infected individuals R^*.

Conclusions

The aim of this work was to calculate, by means of concentration balances and the Wells-Riley infection model, the infection probability in an all-air ducted HVAC system with air recirculation and in a primary air system. After a brief analysis of a simple model (already considered in the specific literature), several improvements to the model were added. The results highlight an important outcome related to HVAC plants with air recirculation: dilution with recirculation in multiple rooms is not enough to compensate for the increased number of involved susceptible individuals. High air renewal rates can strongly reduce the risk of infection at a given recirculation rate; furthermore filtration (or other equivalent technologies, such as UV-C irradiation or ionization, to inactivate the virus from recirculated airflows) is a very powerful tool to reduce the infection probability, especially if coupled with high recirculation rates.

Energy consumption for virus inactivation/removal can't be neglected in the design of operating plants and can vary widely, strongly depending on the equipment. The impact on energy consumption will likely be quite high for traditional physical filtration, and lower for ionization: the designer should consider this issue in detail.

Finally, it is very important to consider, in real-world applications, the management of airflows in both segregated and common spaces, which can heavily modify the performance of the system with respect to infection probability. For online figures and equations, visit https://tinyurl.com/JournalExtras.

References

1. Morawska L., J. Cao. 2020. "Airborne transmission of SARS-CoV-2: The world should face the reality." *Environment International* 139:105730. https://doi.org/10.1016/j.envint.2020.105730.

2. Ai Z.T., A.K Melikov. 2018. "Airborne spread of expiratory droplet nuclei between the occupants of indoor environments: A review." *Indoor Air* 28(4):500-524. https://doi.org/10.1111/ina.12465.

3. Sze To G.N., C.Y.H. Chao. 2010. "Review and comparison between the Wells-Riley and dose-response approaches to risk assessment of infectious respiratory diseases." *Indoor Air* 20 (1):2-16. https://doi.org/10.1111/j.1600-0668.2009.00621.x.

4. Buonanno G., L. Stabile, L. Morawska. 2020. "Estimation of airborne viral emission: Quanta emission rate of SARS-CoV-2 for infection risk assessment." *Environment International* 141:105794. https://doi.org/10.1016/j.envint.2020.105794.

5. Gammaitoni L., M.C. Nucci. 1997. "Using a mathematical model to evaluate the efficacy of TB control measures." *Emerging Infectious Diseases* 3(3):335-42.

6. Buonanno G., L. Morawska, L. Stabile. 2020. "Quantitative assessment of the risk of airborne transmission of SARS CoV-2 infection: prospective and retrospective applications." *Environment International* 145:106112. https://doi.org/10.1016/j.envint.2020.106112.

7. Jimenez J., Z. Peng. 2020. "COVID-19 aerosol transmission estimator." https://tinyurl.com/covid-estimator. ■